

[10]. Biodegradable materials are almost completely used in these environmentally friendly techniques [11]. Furthermore, the characteristics of ZnO NPs may depend on the sources of the plant precursors due to the wide variations in the chemical composition of plant extracts.

Several phytochemicals, including polysaccharides and polyphenols, were reported to be present in almost all plant extracts. These phytochemicals are crucial for functioning as bioreducing and biocapping reagents during the synthesis of ZnO nanoparticles. Zinc oxide has outstanding photochemical reactivity and effectively eliminates pollutants [12].

The aim of this work is to synthesize and characterize new membranes based on nanoparticles and implement hybrid membranes and photocatalytic processes in an integrated system for the degradation of pollutants-containing solutions. Many industrial sectors can use this technology: for the purification of wastewater, in the textile industry, the food industry, and the pharmaceutical sector. As a result, catalytic membrane reactors are considered a potential technology in various industrial fields, including biotechnology, the pharmaceutical sector, petrochemicals, chemical plants, energy, and environmental applications. This process is an innovative alternative for sustainable growth that depends on the design strategy to gain benefits in manufacturing and processing. (i) Synthesis of membranes coupled with nanoparticles to use in-situ photocatalytic processes was tested for the first time in the degradation of pollutants, (ii) Application of an integrated treatment system. The integrated system will lead to the implementation of processes in biotechnology, the pharmaceutical sector, petrochemicals, chemical plants, energy, and environmental applications. The system eventually aims for the recovery of water sources from effluents and the re-use of water back into the industrial process system. The incorporation of membrane techniques into the treatment processes of liquid effluents loaded with metal ions has emerged. Filtration membranes (microfiltration, ultrafiltration, nanofiltration, reverse osmosis, pervaporation, and electro-membrane techniques) would be used for this purpose with questionable efficiency and selectivity. Indeed, many industrial sectors use this technology: for the purification of wastewater, in the textile industry, the food industry, and the pharmaceutical sector. Recently, significant research efforts have been devoted to catalytic membrane reactors, as types of membrane reactors, considered multifunctional catalytic reactors fusing membrane-based separation and chemical reaction into a single unit. Proper design of the catalytic membrane reactor leads to improved efficiency, reagent conversion, and lower downstream separation costs.

The purpose of this work is to depollute wastewater using membrane ultrafiltration technology. The present study was designed to test the following hypotheses: (1) The catalytic properties of biodegradable materials resulting from the green synthesis process;

(2) The treatment method by ZnO NPs coupled with CA membranes has reliability and efficiency in depolluting organic and mineral contaminants.

Materials and Methods

Materials: Methyl orange, polyethylene glycol (PEG 1000), and dimethylformamide (DMF) (CAS 68-12-2) and CA (CAS 9004-35-7) were given by Dae-Jung Chemicals and Sigma-Aldrich, respectively. The addition of HCl (0.1 M) and NaOH (0.1 M) solutions kept the pH of the solution at the desired levels. All prepared solutions were made with distilled water, and all experiments were carried out at room temperature.

Plant collection and extraction: Fresh fenugreek plant leaves were brought into the laboratory. To eliminate attached particles, the plant leaves were carefully cleaned with tap water and then washed with distilled water. In a glass beaker, 20 grams of leaves were heated through 100 ml of deionized water for 30 min at 80°C. After cooling the extract, it was filtered through Whatman filter paper. The leaf extract was stored in a refrigerator for further ZnO-NP synthesis.

Green synthesis process: The aqueous extract of the plant was used to reduce zinc to ZnO NPs. Briefly, a heated stirrer was used to boil twenty milliliters of fenugreek aqueous leaf extract at 60-80°C. Once the extract attained 100°C, 5 g of zinc sulfate heptahydrate ($\text{Zn}(\text{SO}_4)_2 \cdot 7\text{H}_2\text{O}$) was added. The above solution was heated at the same temperature until it was lowered to a light yellowish paste. The paste was introduced dropwise into a ceramic crucible, located in a muffle furnace, and dried and calcined for 3 hours at 300°C. As a result, a dry, pale yellowish powder was formed.

AC/ZnO UF membrane preparation: Synthesis of a membrane coupled with ZnO NPs was performed according to the method described by Alhalili et al. [13].

Photocatalytic Activity: To test the photocatalytic activity of ZnO NPs, we add 25 ppm Malachite dye to 100 mL of distilled water. The initial concentration (20 mL) was removed from the solution, and the remaining solution of 0.1 g of ZnO-NPs catalyst was added to 80 mL of dye solution. To maintain the adsorption-desorption equilibrium, the solution was installed in the dark for 30 minutes, afterward exposed to UV light, and samples were taken every 15 minutes. To remove the catalyst from the samples, centrifugation at 10.000 rpm for 15 minutes was used. The degradation of dye was monitored using a UV visible spectrophotometer. The removal rate of dye was estimated using the following formula (Eq. 1):

$$\% = \frac{(C_0 - C)}{C_0} * 100 \quad (1)$$

Where C_0 is the initial concentration of the dye and C is the concentration after a time interval.

SPSS v17. The mean difference comparison between the treatments was analyzed by t-test or analysis of variance (ANOVA) and subsequently by the Tukey HSD test at $P < 0.05$.

Results and Discussion

ZnO Nanoparticles (NPs) Characterization

In the present study, a color shift from yellowish to white designed the formation of ZnO NPs through fenugreek leaf extracts. Zn ions were converted to

ZnO NPs by flavonoids and phenolic compounds. The solution's color suddenly changed after several hours, revealing that the ZnO salt had been completely bioreduced into NPs (Fig. 1). The structural characteristics of the synthesized ZnO NPs were defined using an X-ray diffractometer, which is employed to determine the nanoparticles' ZnO structure phase. As shown in Fig. 2A, the X-ray diffraction pattern of zinc oxide nanoparticles demonstrates distinct line broadening of the X-ray diffraction peaks, suggesting that the obtained powder was of nanometric size. In addition, the XRD pattern of ZnO NPs demonstrates an intense peak that clearly shows the purification

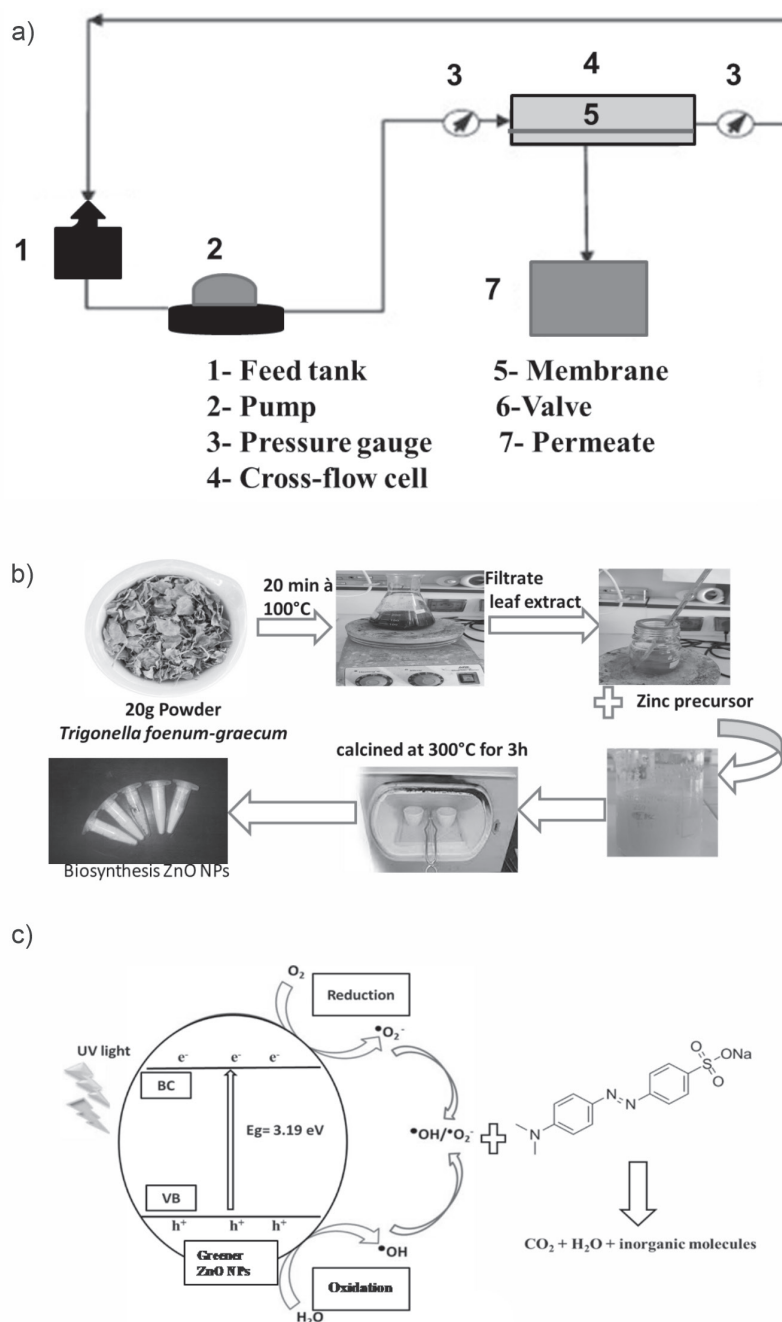


Fig. 1. a) Ultrafiltration experimental system, b) Green synthesis of zinc oxide nanoparticles using fenugreek, and c) Plausible degradation mechanisms.

the degradation is fast in the first 15 minutes and achieves 92% color removal after around 30 minutes of irradiation. By increasing the number of active sites on the photocatalyst surface, which also increases the amount of hydroxyl and superoxide radicals, the % of dye removal increases as ZnO concentration increases [28, 29].

Initial Dye Concentration Effect

A similar experiment was carried out by maintaining the dose of catalyst stable while increasing the concentration of dye solution from 25 mg/L to 75 mg/L (Fig. 3D). All experiments (except for 75 mg/L) achieved nearly 96% color removal. The degradation rate was considerably affected by dye concentration. As a result, for the remaining photodegradation percentages of nanoparticle ZnO NPs, the dye concentration was fixed at 25 mg/L. As an outcome, it is expected that increasing the concentration of MO will enhance with oxidizing agents, improving the degradation process. In contrast, the efficiency of the dye's degradation increases as the initial concentration increases [17].

Plausible mechanisms: By incorporating micrometer and nanometer sized inorganic oxide particles into the polymeric casting solution or by synthesizing them on-site, organic-inorganic hybrid membranes can be made. Few researchers have noted the combination of organic polymers with inorganic substances such as alumina, titanium, silica, etc. The assembly of engineered nanoparticles on the surface of porous membranes or the mixing of them with polymeric casting solution are two methods used in recent years to construct nano inorganic mixed matrix membranes. The type of attachment bonds between the polymer chains and inorganic phases in the composite fabric, as well as the degree of cross-linking of the polymeric matrix, will affect the membrane's structure. We have focused on creating inexpensive, inorganic membranes with a decent yield and performance as their main characteristics. During the manufacture of membranes, interactions between the surface of nanoparticles and polymer chains and/or solvents result in membranes with the desired structure. These structural alterations produce optimal selectivity and permeability for gas separation as well as adequate performance in membranes for nano and ultrafiltration. The other goal is to control membrane fouling that is brought on by hydrophilic functional groups of nanoparticles. The inorganic phase's presence can also be employed to limit the polymer chains' molecular motions and increase the mean distance between them. Limited molecular movements and a favorable rise in the mean distance between chains can lead to simultaneous improvements in membrane porosity, stability, and performance. Fig. 1C depicts the plausible photocatalytic degradation mechanism of MO by ZnO NPs under UV light. Once the ZnO NPs were exposed to UV light, conduction band electrons (e⁻) and valence band holes (h⁺) were established on the

catalyst's surface. The holes formed extremely reactive hydroxyl radicals (\bullet OH) when they reacted with water, while oxygen created a superoxide radical anion (\bullet O₂⁻). As an outcome, the strong radicals \bullet OH and \bullet O₂⁻ were primarily responsible for the degradation and fading of MO dye, as published in many previous papers [18, 19]. Therefore, the ZnO NPs' large surface area resulted in excellent photocatalytic activity.

Membrane Characterization

Fourier Transform-Infrared Spectroscopy Analysis

Although IR spectroscopy is a very potent characterization method for detecting chemical groups and gaining a plethora of microscopic information on their conformation and potential interactions, it was employed to confirm the impact of biosynthesized ZnO NPs on the vibration characteristics of membranes. The FTIR spectra of CA nanocomposite membranes (M0 and M1) are shown in Fig. 4A). ZnO NPs were incorporated as a modifier oxide. DMF and PEG 1000 were used as additives in the matrix (i.e., CA). The addition of ZnO NPs is intended to improve the thermal properties, hardness, and density of the membranes. We observed the emergence of a high-intensity wide band in the wave number range of 2900-3500 cm⁻¹. The band might be related to the hydroxyl groups' stretching vibration [30]. Additionally, a medium-intensity band that appears at 720 cm⁻¹ is connected to the stretching vibrations of Zn-O [13].

Water Contact Angle Measurement

One of the crucial characteristics of membranes that could have an impact on their ability to flow and resist fouling is their surface hydrophilicity. As shown in Fig. 4B), the addition of ZnO NP regularly reduces the contact angle of the integrated membranes. The presence of biosynthesized nanoparticles increased the hydrophilicity of the membranes because the low angle of contact indicated a high hydrophilicity. The contact angle was reduced from 86° to 50° for membranes composed of CA complexed with 0.05 g of ZnO NPs. Other studies have shown that the presence of nanoparticles induces a lower aggregation and high hydrophilicity [13, 31].

Water content and porosity study: The results of Fig. 4C) show that the addition of ZnO increases the porosity. Gaps are created in the polymer matrix due to the separation of the polymer chains caused by the presence of NPs, which increases the water flow. The ZnO oxide induces the hydrophilicity of the membrane surface [13, 32].

Scanning Electron Microscopy (SEM) Analysis

The images emitted from the cross section and the upper surface are presented in Fig. 5A). The shape of

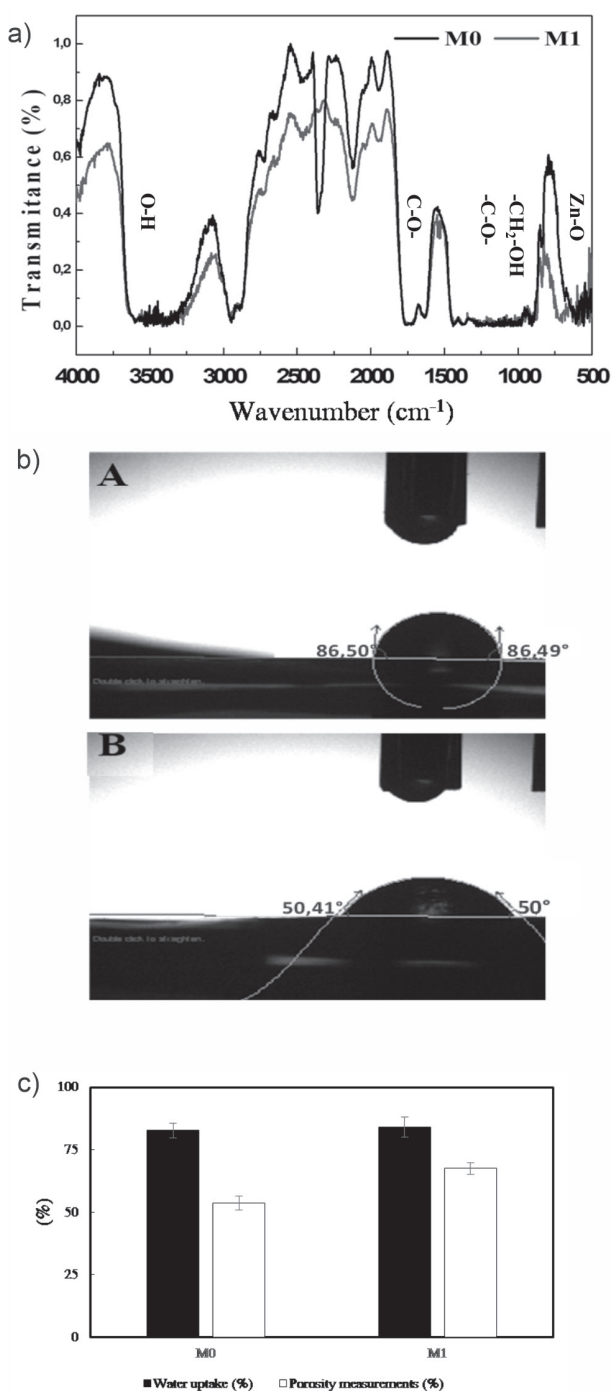


Fig. 4. A) Infrared (IR) spectrum, B) Water contact angle, and C) Water uptake (%) and porosity measurements (%) of the bare and the nanocomposite membranes without ZnO NPs (M0), CA membrane with ZnO NPs (M1).

the cellulose membranes is asymmetric and contains a dense layer supported on a porous substructure with macro-voids, although both surfaces are homogeneous, smooth, and dense. The upper layers of the membranes control the rejection and limit the flow [13]. The pores are numerous in the membrane layers rich in ZnO NPs compared to the controls.

Water permeability: In terms of water permeability, the performance of the membranes was analyzed. The

results of water flow as a function of pressure are presented in Fig. 5B). The water flow depends on the pressure in accordance with Darcy's law. The water permeability for the tested membranes (M0) = 9.4596 L h⁻¹ m⁻² bar⁻¹ and (M1) = 21.501 L h⁻¹ m⁻² bar⁻¹ were determined. This permeability represents the initial state of the membranes. The flow increased linearly with the pressure, and the membrane had a lower flow rate than the membrane rich in ZnO NPs.

Filtration of Dyes

Pressure Effect

The effect of the transmembrane pressure on the retention and flow of Malachite permeate (50 mg L⁻¹) was determined for pressures varying from three to six bars using membranes rich or not in ZnO NPs. The pressure has a significant effect on dye retention (Fig. 6IA). The permeate flow rate increased proportionally with the pressure (Fig. 6IB). A higher permeate flow rate would result from a higher permeate pressure [33, 34].

Ionic Strength Effect

The effectiveness of treatment techniques such as adsorption or biological treatment was generally affected by the presence of different substances, such as salts, acids, and alkalis, in textile effluents. The variation in the retention rate of the Malachite and the permeate flow in the presence of different concentrations of NaCl affects the efficiency of the ultrafiltration process. The dye concentration was fixed at 50 mg L⁻¹, the NaCl content varied from 0.3 to 1.1 g L⁻¹, and the pressure was constant at four bars. When the NaCl concentration increased, the retention rates of the Malachite anionic dye significantly decreased (Fig. 6IIA). It seems that the electrostatic interaction between the dye molecules and the membrane surfaces with many charged groups is reduced when there is a high concentration of NaCl. The NaCl content significantly affects the permeate flow (Fig. 6IIB). As previously described, during the membrane complexation process with the dye, the chloride ions compete with the anionic dye [35].

ph Effect

The pH value affects the level of ionization of the dye. This could have an impact on the stability of the complex and, consequently, on the dye retention rate. The pH varies from 3 to 11, the dye concentration is 50 mg L⁻¹, and the transmembrane pressure value is about 4 bars. It can be seen from Fig. 6IIIA) that for the pH levels of 3 and 7, the rates of Malachite rejection varied from 78 to 100%. The removal of the Malachite decreases for M0 and M1 from pH = 9. For this reason, it is necessary to take into account the electrostatic interactions between the charged dye molecules

